



The background features a detailed line art illustration of a river ecosystem. It includes several fish of different species, some with spots, swimming in the water. There are also water lilies with large, open flowers and long stems. A small insect, possibly a damselfly nymph, is shown near the surface. The overall style is clean and technical, using only blue outlines on a white background.

# Joint Danube Survey 3

Summary report on  
Radioactivity



## Authors

Franz Josef Maringer, Claudia Ackerl, Andreas Baumgartner,  
Christopher Burger-Scheidlin, Maria Kocadag, Johannes H. Sterba,  
Michael Stietka, Jan Matthew Welch

## Imprint

Published by:

ICPDR – International Commission for the Protection of the Danube River

© ICPDR 2017

Contact

ICPDR Secretariat

Vienna International Centre / D0412

P.O. Box 500 / 1400 Vienna / Austria

T: +43 (1) 26060-5738 / F: +43 (1) 26060-5895

[icpdr@unvienna.org](mailto:icpdr@unvienna.org) / [www.icpdr.org](http://www.icpdr.org)



# Table of contents

## 1. Introduction 4

## 2. Methods 6

2.1	Low-level gamma-ray spectrometry	6
2.2	Strontium-90 radiochemical analytics	6
2.3	Extraction method	6
2.4	Assessment of the extraction yield	6
2.5	Radiochemical separation	7
2.6	Strontium-90 analytics by Liquid Scintillation Counting	7
2.7	Colour quench corrections	7

## 3. Results 8

3.1	Potassium-40	9
3.2	Caesium-137	10
3.3	Radium-228 and Thorium-228	11
3.4	Uranium-238, Radium-226 and Lead-210	12
3.5	Radium-228 / Radium-226	13
3.6	Caesium-137 levels between 1988 and 2013	14
3.7	Strontium-90	16
3.8	Discussion of Strontium-90 analysis uncertainties	16

## 4. Conclusions 17

## 5. References 18



# 1. Introduction



Highly elevated levels of artificial and / or natural radionuclide concentration in rivers lead to increased health risk of population which drink (purified) river water or consume contaminated river fish. Additionally the use of contaminated river water for irrigation purpose of agricultural areas could increase the health risk by consumption of the products produced on these areas. Therefore it is of relevance to investigate periodically the radioecological status of the Danube river ecosphere to assess the public health impact of radionuclides on the population living in the Danube basin (Frantz, 1967; Rank, 1976; Tschurlovits, 1980).

$^{90}\text{Sr}$  and  $^{137}\text{Cs}$  activity concentrations (half-life 28,8 yr and 30,2 yr respectively) in Danube water and solid particles originated primarily from the nuclear power plant accident in Chernobyl (April, May 1986) and secondarily from atmospheric nuclear weapons test fallout during the 1950s and 1960s.

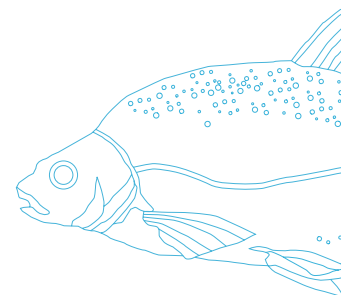
Major natural occurring radioactive constituents of the earth's crust are the isotopes  $^{238}\text{U}$  (half-life  $4,5 \cdot 10^9$  yr) and  $^{232}\text{Th}$  (half-life  $14,1 \cdot 10^9$  yr) and their radioactive decay nuclides (e.g.  $^{210}\text{Pb}$ ,  $^{226}\text{Ra}$ ,  $^{228}\text{Ra}$ ,  $^{228}\text{Th}$ ). Being created during the cosmic formation of the elements in a supernova and then building the earth's matter, these radioisotopes, due to their extremely long physical half-life, now can be found in almost every sort of rock and its weathering product, the soil. The ubiquity of these radioisotopes also implies the presence of its decay nuclides in rocks and soil like  $^{226}\text{Ra}$  ( $T_{1/2} = 1,6 \cdot 10^3$  yr), and  $^{228}\text{Ra}$  ( $T_{1/2} = 5,7$  yr) respectively.

The levels of natural ( $^{40}\text{K}$ ,  $^{210}\text{Pb}$ ,  $^{226}\text{Ra}$ ,  $^{228}\text{Ra}$ ,  $^{228}\text{Th}$ ,  $^{238}\text{U}$ ) and artificial ( $^{137}\text{Cs}$ ,  $^{90}\text{Sr}$ ) radionuclide concentrations of 65 sediment samples, collected during the joint survey cruise JDS3 in summer 2013 (ICPDR, 2015) in the Danube and the main tributaries have been radiometrically analysed.  $^{226}\text{Ra}$  and  $^{228}\text{Ra}$  analysis of sediment allow identifying the geochemical background, the influence of mining industry as well as changing sediment sources.

**Table 1: Sediment samples analysed on radioactivity**

Sample Nr.	Date	River km	Lab Code
JDS 1 L	13.08.2013	2581	G9946
JDS 2 M	13.08.2013	2415	G9947
JDS 3 M	14.08.2013	2354	G9948
JDS 4 M	15.08.2013	2285	G9949
JDS 5 M	16.08.2013	2258	G9950
JDS 6 M	17.08.2013	2205	G9951
JDS 7 M	18.08.2013	2120	G9952
JDS 8 M	18.08.2013	2008	G9953
JDS 9 M	19.08.2013	1942	G9954
JDS 10 M	20.08.2013	1985	G9955
JDS 11 M	21.08.2013	1881	G9956
JDS 13 M	21.08.2013	1869	G9957
JDS 14 M	22.08.2013	1852	G9958
JDS 15 M	23.08.2013	1806	G9959
JDS 16 M	23.08.2013	1794	G9960
JDS 17 M	23.08.2013	1790	G9961
JDS 18 M	24.08.2013	1766	G9962
JDS 19 M	24.08.2013	1761	G9963
JDS 20 M	25.08.2013	1707	G9964
JDS 21 M	25.08.2013	1660	G9965
JDS 22 M	26.08.2013	1632	G9966
JDS 24 M	28.08.2013	1560	G9967
JDS 25 M	29.08.2013	1533	G9968
JDS 26 M	29.08.2013	1481	G9969
JDS 27 M	30.08.2013	1434	G9970
JDS 28 M	31.08.2013	1384	G9971
JDS 29 M	31.08.2013	1379	G9972
JDS 30 M	31.08.2013	1367	G9973
JDS 31 M	01.09.2013	1300	G9974
JDS 32 M	02.09.2013	1262	G9975
JDS 33 M	03.09.2013	1252	G9976
JDS 34 M	03.09.2013	1216	G9977
JDS 35 M	03.09.2013	1215	G9978
JDS 36 M	04.09.2013	1200	G9979
JDS 37 M	04.09.2013	1170	G9980
JDS 38 M	06.09.2013	1159	G9981
JDS 39 M	06.09.2013	1151	G9982
JDS 40 M	07.09.2013	1107	G9983
JDS 41 M	07.09.2013	1103	G9984
JDS 42 M	07.09.2013	1097	G9985

Sample Nr.	Date	River km	Lab Code
JDS 43 M	08.09.2013	1071	G9986
JDS 44 M	09.09.2013	1040	G9987
JDS 45 M	09.09.2013	954	G9988
JDS 46 M	10.09.2013	926	G9989
JDS 47 M	12.09.2013	851	G9990
JDS 48 M	12.09.2013	845	G9991
JDS 49 M	13.09.2013	834	G9992
JDS 50 M	14.09.2013	685	G9993
JDS 51 M	14.09.2013	637	G9994
JDS 52 M	15.09.2013	602	G9995
JDS 53 M	15.09.2013	550	G9996
JDS 54 M	16.09.2013	537	G9997
JDS 55 M	16.09.2013	532	G9998
JDS 56 M	16.09.2013	498	G9999
JDS 57 M	18.09.2013	488	G10000
JDS 59 M	19.09.2013	429	G10001
JDS 60 M	19.09.2013	378	G10002
JDS 61 M	20.09.2013	235	G10003
JDS 62 M	21.09.2013	167	G10004
JDS 63 M	22.09.2013	154	G10005
JDS 64 M	22.09.2013	135	G10006
JDS 65 M	22.09.2013	130	G10007
JDS 66 M	24.09.2013	18	G10008
JDS 67 M	25.09.2013	26	G10009
JDS 68 M	25.09.2013	107	G10010



# 2. Methods

## 2.1 Low-level gamma-ray spectrometry

The radiometric analysis of the homogenized and frozen dried sediment samples (grain size fraction  $< 63 \mu\text{m}$ ) was carried out by low-level gamma-spectrometry. By this method, which was carried out with three low-level Germanium detectors in a specially shielded laboratory (Low-level Counting Laboratory Arsenal, Vienna), the activity concentration of the gamma emitting radionuclides in the samples was analysed. The radiometric equipment consists of a coaxial low-level HP-Ge-detector (BSI, 50 % rel. efficiency) detecting gamma energies between 30 to 2800 keV. Calibrations of the detectors were carried out by NIST-, IAEA-, and PTB-standard reference materials. The calculations of the radionuclide concentrations and data handling were done by BSI Spectroscopy System and software developed by the departmental research group.

Because of the relatively low radioactivity concentrations, long counting periods (24 to 72 hours) were necessary to obtain reasonable counting statistics for all radionuclides of interest.

## 2.2 Strontium-90 radiochemical analytics

The activity concentration of  $\beta$ - emitting  $^{90}\text{Sr}$  in the sediment samples (grain size fraction  $< 63 \mu\text{m}$ ) from 65 locations along the Danube river was determined. The yield of strontium extracted from the geological matrix was determined by total reflection X-ray fluorescence (TXRF).  $^{90}\text{Sr}$  was then processed radiochemically, separated with strontium-selective resins and quantified by liquid scintillation counting (LSC).

## 2.3 Extraction method

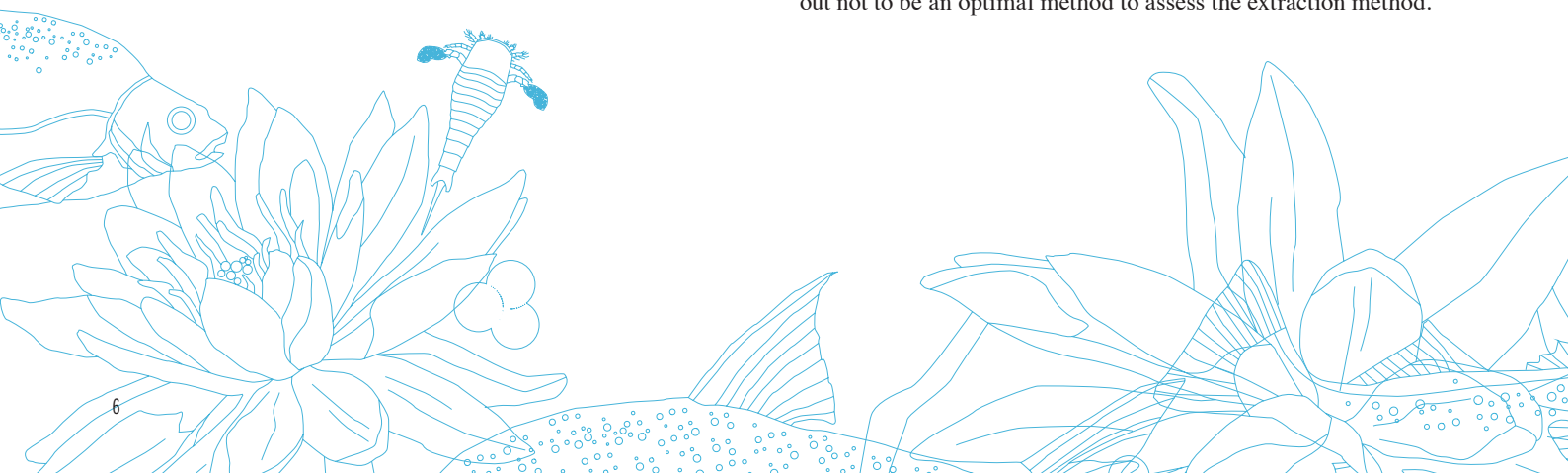
The sediment samples (2,00 g) were weighed into a round-bottomed flask (10 mL). Concentrated (14,8M)  $\text{HNO}_3$  (2,5 mL), distilled water (2,5 mL) and 30%  $\text{H}_2\text{O}_2$  (1 ml) were added, reflux condenser was mounted, and the flask was heated for 30 minutes on a boiling water bath (Mundschenk, 1994). The hot solution was filtered and the round-bottomed flask was washed 5 times with 1 ml 8M  $\text{HNO}_3$  which was also subsequently filtered. The filtrate (extractant and washings) was collected and set aside, while the solid residue was scraped from the filter paper into a 10 ml round-bottomed flask. The extraction and washing procedure was repeated twice more, resulting in three liquid fractions of extractant and washing from each cycle in three separate vessels.

## 2.4 Assessment of the extraction yield

### ICP-MS

From each sample, 1 ml was pipetted into an ICP-MS test tube and diluted further with 9 ml distilled water and measured for caesium ( $m/z = 137$ ), barium ( $m/z = 137,138$ ), strontium ( $m/z = 84,85,87,88,90$ ) and iron ( $m/z = 56$ ). Due to observed detector saturation, more dilute samples (100  $\mu\text{l}$  sample in 10 ml water) were prepared. The whole experiment was repeated with a sample spiked with a strontium nitrate solution (c: 1,2 mg/ml) and dried overnight in an oven at 30–35°C.

Due to spectroscopic interferences, no sensible results could be achieved. Spectroscopic interferences are interferences, which are produced after the atomization of the sample. ICP-MS turned out not to be an optimal method to assess the extraction method.



### TXRF measurements

For a TXRF (Total Reflection X-ray Fluorescence) test measurement, one sediment sample was prepared with a digestion (heating) time of one hour. To generate useable TXRF data, the concentration of iron in the solution needed to be balanced against the strontium concentration to prevent oversaturation by iron signals. Strontium in the samples was successfully quantified by (TXRF). The measurements revealed that after one hour digestion time 90% of the strontium was dissolved and after 2 hours 98%. It is assumed that after 2 hours of cooking, strontium is nearly quantitatively extracted from the soil, especially  $^{90}\text{Sr}$  which should only be present on the surface of the sediment grains.

### 2.5 Radiochemical separation

Extractions were carried out as described, but with the addition of 0,5 ml of  $\text{Sr}(\text{NO}_3)_2$ -solution (1,2 mg/ml) and 2 hours heating time (single extraction per sample). Afterward the solutions were evaporated to dryness on a hotplate and the residue was put into a vessel, sealed and labelled. Prior to radiochemical isolation of Strontium, the residue was taken up in 4 ml 8M  $\text{HNO}_3$ .

For the separation of the strontium from other radionuclides, crown-ether (4,4'(5')-di-t-butylcyclohexano 18-crown-6) – based strontium-selective resins were used (Horwitz, 1991; Pimpl, 1995; Kocadag et al., 2013; <http://www.eichrom.com/>). About 350 mg of resin were weighed into a disposable plastic column and preconditioned with 5 ml 8M  $\text{HNO}_3$  for at least 1,5 hours. Excess acid was then eluted from the column and a frit applied to the top of the column. The solution with the sample was applied to the resin and the beaker containing the sample was washed twice with 1 ml 8M  $\text{HNO}_3$  which was also loaded onto the resin. The loaded resin was washed with 5 ml of a solution with 3M  $\text{HNO}_3$  and 0,05M oxalic acid to elute ions other than strontium. In the next step, the strontium was eluted from the column with 10 ml 0,01 M  $\text{HNO}_3$  and the resulting fraction was then evaporated to dryness.

### 2.6 Strontium-90 analytics by Liquid Scintillation Counting

The residue was taken up in 1 ml 0,01M  $\text{HNO}_3$  and pipetted into a LSC-vial. The beaker that had contained the residue was subsequently washed three times with 1 mL 0,01M  $\text{HNO}_3$  to assure that all of the strontium eluted was transferred from the beaker into the vial. To the 4 ml Sr-solution, 16 ml of the scintillation cocktail „UltimaGold” were added and shaken, resulting in a viscous and limpid solution.

### 2.7 Colour quench corrections

Since the samples prepared have a yellowish colouration, which presumably resulted from organic substances, a correction for the effects of this colouration on LSC counting efficiency must be made. In this case  $\text{K}_2\text{CrO}_4$  or  $\text{K}_2\text{Cr}_2\text{O}_7$  may be used to imitate the colouration of the samples and account for the effect of colour quenching on the LSC results. A correction for colour quenching may be applied by measuring a series of standard samples of known activity of  $^{90}\text{Sr}$  with different amounts of colourant. When each sample has been counted, a curve (quench curve) is produced showing the relation between tSIE (transformed Special Index of External standard spectrum) and count efficiency (on the basis of the known activity). The quench curve produced shows that counting efficiency is only effected by very strong colouration (as measured by tSIE). Since none of the samples of sediment extract was strongly coloured, colour quenching does not significantly influence the results of sample counting.

The first five samples were counted for 1000 minutes (~17 h), but it was decided to decrease the measuring time to 700 minutes (~12 h) such that two samples per day could be measured with measurement uncertainties below 2%.

# 3. Results

The Danube can be separated into three larger geomorphological segments to be able to present the measured results in greater detail. Those parts are the 1. Northern Alpine Forelands and Vienna Basin (upper section), 2. the Pannonian lowland (middle section), and 3. the Walach lowlands (lower section).

The upper section reaches from the river's origin to the Hainburger Gate, the middle section from the Hainburger Gate to the Iron Gate, and the lower section from the Iron Gate to Sulina.

The Hainburger Gate is located at the Austrian/Slovak border and the river stretch observed was defined between Danube River kilometres 2857 and 1880. Starting at river kilometre 1880, the middle section goes as far as the Iron Gate, which however, is over 80 km long. Therefore, the centre at Danube river km 904 was chosen as a compromise. The last section starts at the Iron Gate and ends at the Black Sea.

In all the graphs, the main tributary rivers of the Danube were indicated to explain possible changes to certain isotope activities that may be caused by the additional radioactivity input or dilution.





### 3.1 Potassium-40

The potassium radionuclide  $^{40}\text{K}$  is naturally found all over the planet and represents only a very small fraction (0,012%\*) of the total amount of potassium in the environment.

Fig. 1, Fig. 2, and Fig. 3 show the results from the measurements of the nuclide.

An increasing trend in the amount of radioactive potassium can be observed the closer the sampling locations were to the Black Sea. A quite noticeable result was retrieved at river kilometre locations 1170 and 1159, where the level of  $^{40}\text{K}$  was significantly lower than anywhere else on the entire length of the Danube. At 1159 the result was below the detection limit of 51 Bq/kg.

Fig. 1:  $^{40}\text{K}$  between river kilometre 2581 and 1880

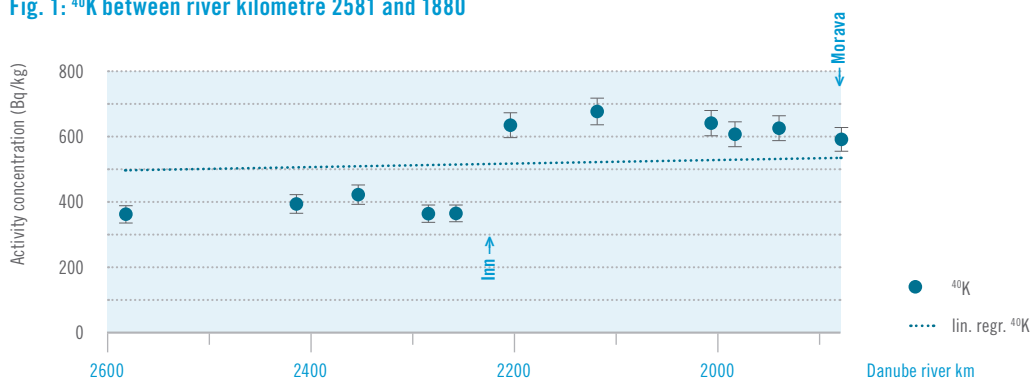


Fig. 2:  $^{40}\text{K}$  between river kilometre 1880 and 904

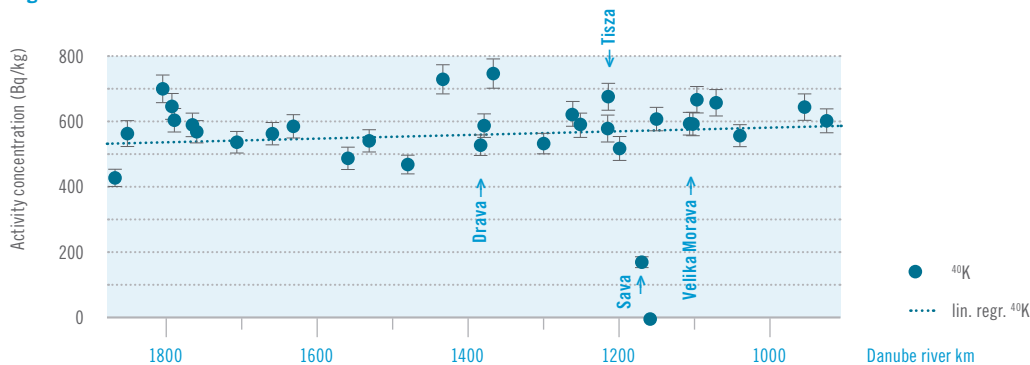
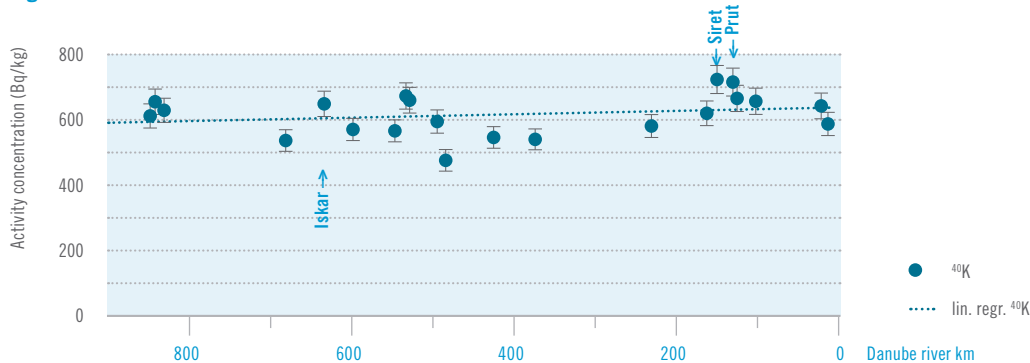


Fig. 3:  $^{40}\text{K}$  between river kilometre 904 and 0



\* c.f. National Institute of Standards and Technology, 2016a.

### 3.2 Caesium-137

$^{137}\text{Cs}$  is a radioactive isotope with a half-life of 30,17 years\* and does not occur naturally. The measured levels can be traced back to the nuclear accident of the Chernobyl reactor in 1986 as well as atmospheric nuclear tests conducted during the 1950s and 1960s.

A decrease in Caesium levels can be seen from the performed linear regression of the data in Fig. 4, Fig. 5, and Fig. 6. This is due to the development and distribution of the radioactive plume in the days after the Chernobyl disaster with winds blowing west towards central and northern Europe and the subsequent precipitation. Another contributing factor is the dependence on the composition of the bottom sediment.

Fig. 4:  $^{137}\text{Cs}$  between river kilometre 2581 and 1880

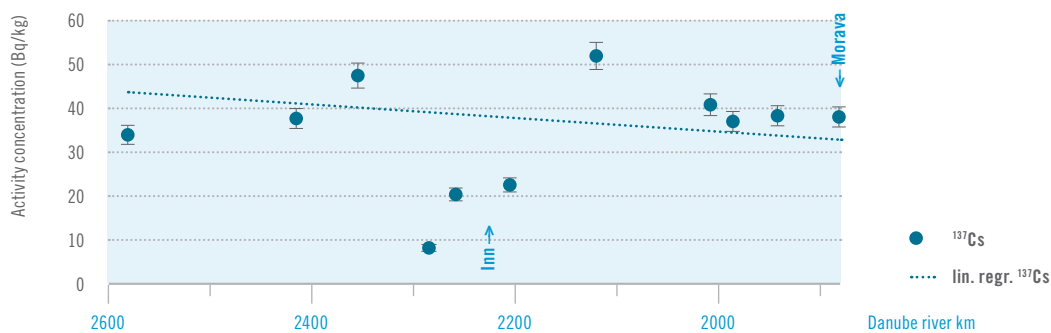


Fig. 5:  $^{137}\text{Cs}$  between kilometre 1880 and 904

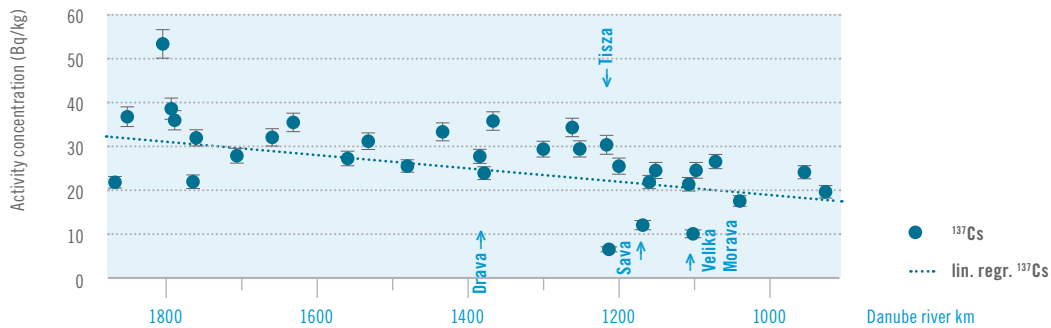
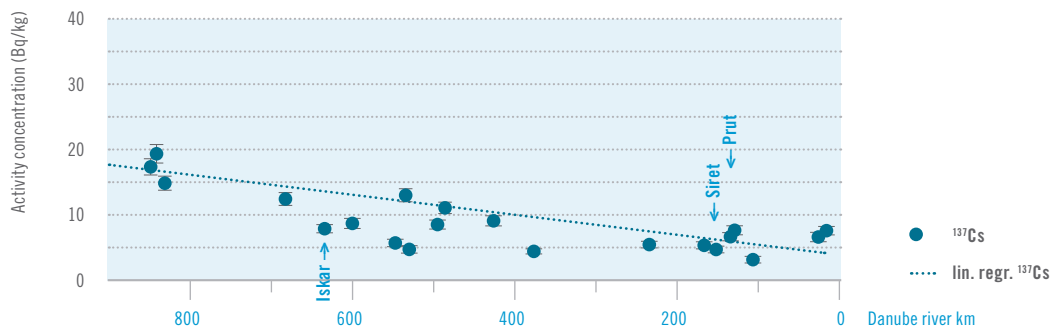


Fig. 6:  $^{137}\text{Cs}$  between river kilometre 904 and 0



\* c.f. National Institute of Standards and Technology, 2016c.

### 3.3 Radium-228 and Thorium-228

Both  $^{228}\text{Ra}$  and  $^{228}\text{Th}$  can be found in the natural thorium decay chain with  $^{228}\text{Ra}$  decaying via a beta ( $\beta$ ) decay to  $^{228}\text{Ac}$  and another beta decay to  $^{228}\text{Th}$ . As a result, similar outcomes were expected when comparing the two radionuclides. Because of the comparably long half-life of  $^{228}\text{Ra}$  it is often used as a monitoring tracer in water quality assessment, since many

consecutive isotopes have relatively short half-lives and their presence is hard to measure accurately without significant efforts.\*  $^{228}\text{Th}$  is one of the radioactive elements in the sequence which takes longer to decay and can thus be detected more easily. The results of activity concentrations measurements of these radionuclides are shown in Fig. 7, Fig. 8, and Fig. 9.

Fig. 7:  $^{228}\text{Ra}$  and  $^{228}\text{Th}$  between river kilometre 2581 and 1880

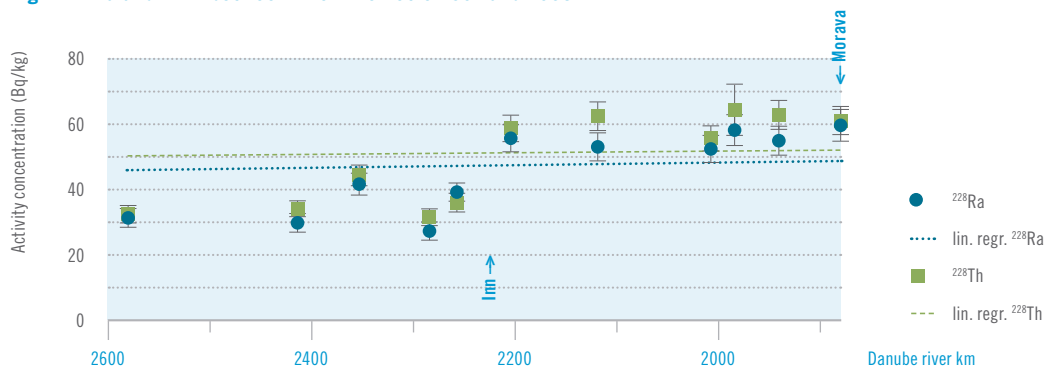


Fig. 8:  $^{228}\text{Ra}$  and  $^{228}\text{Th}$  between river kilometre 1880 and 904

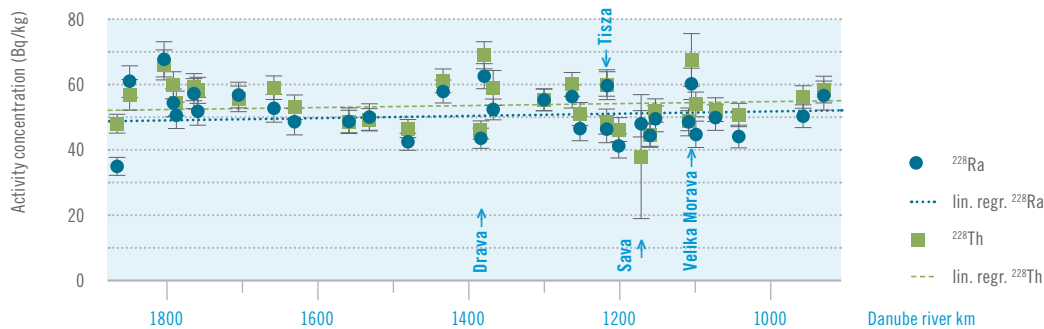
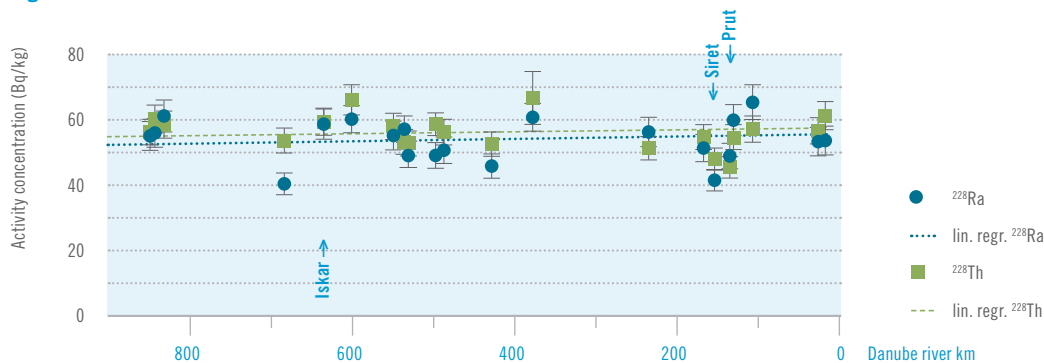


Fig. 9:  $^{228}\text{Ra}$  and  $^{228}\text{Th}$  between river kilometre 904 and 0



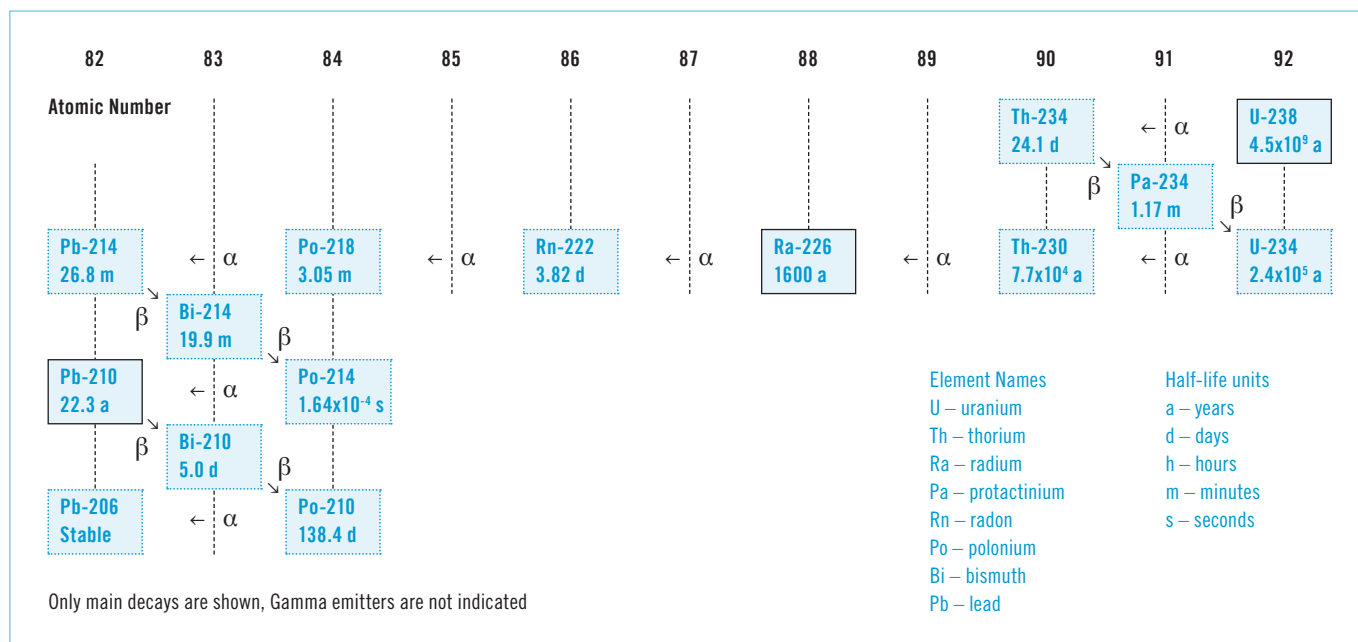
\* c.f. National Institute of Standards and Technology, 2016b.

### 3.4 Uranium-238, Radium-226 and Lead-210

The isotopes  $^{238}\text{U}$ ,  $^{226}\text{Ra}$  and  $^{210}\text{Pb}$  are part of the natural uranium-radium decay chain (Fig. 10). The hereby examined radionuclides have been emphasised with black frames.



Fig. 10: The natural uranium-radium decay chain



The radioactive elements from the series have become important in understanding erosion and chemical weathering.

The activities and ratios between nuclides (Fig. 11, Fig. 12, and Fig. 13) can be used as an indicator of the previously stated processes.\*

Fig. 11:  $^{238}\text{U}$ ,  $^{226}\text{Ra}$  and  $^{210}\text{Pb}$  between river kilometre 2581 and 1880



\* c.f. Dossetoa, et al., 2008.

Fig. 12:  $^{238}\text{U}$ ,  $^{226}\text{Ra}$  and  $^{210}\text{Pb}$  between river kilometre 1880 and 904

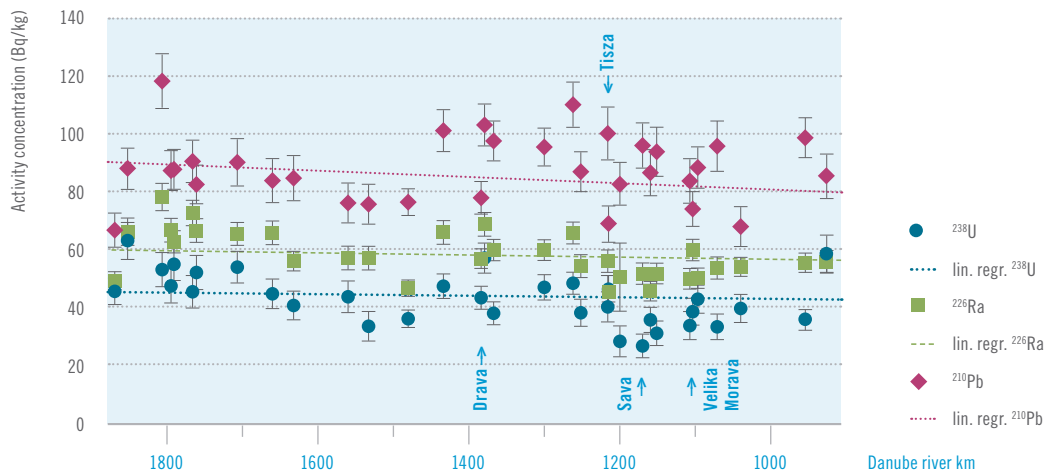
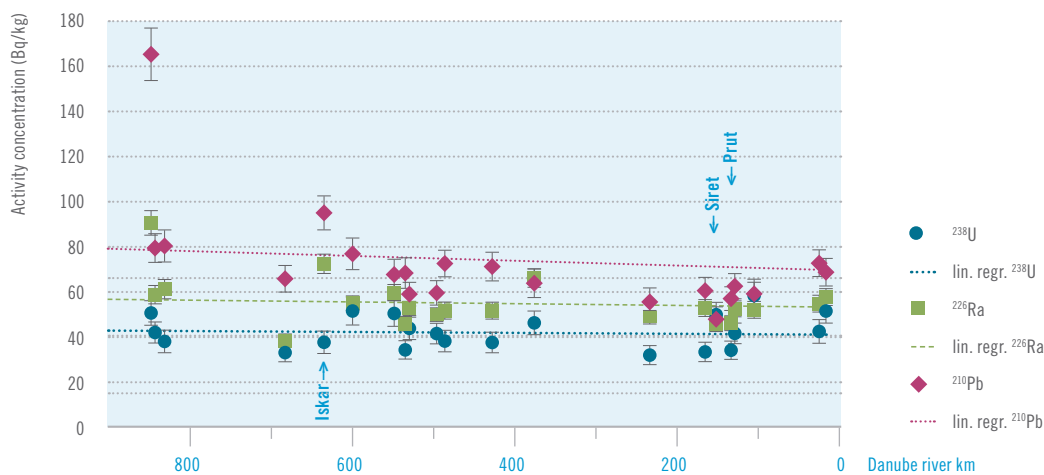


Fig. 13:  $^{238}\text{U}$ ,  $^{226}\text{Ra}$  and  $^{210}\text{Pb}$  between river kilometre 904 and 0



### 3.5 Radium-228 / Radium-226

Fig. 14, Fig. 15, and Fig. 16 show the ratio in which  $^{228}\text{Ra}$  and  $^{226}\text{Ra}$  are present on the length of the Danube. It is commonly used as indicator for source particles, since, as was previously discussed, the isotopes origin from two different decay series, the thorium and uranium-radium series, respectively.\*

Generally, a tendency towards an increase in the ratio can be found when advancing downstream. Values between 0,8–1,0 in the middle section of the Danube can be observed, with some higher ratio results towards the mouth of the river.

\* c.f. Maringer, et al., 2009, pp. 6–7.

Fig. 14:  $^{228}\text{Ra} / ^{226}\text{Ra}$  between kilometre 2581 and 1880

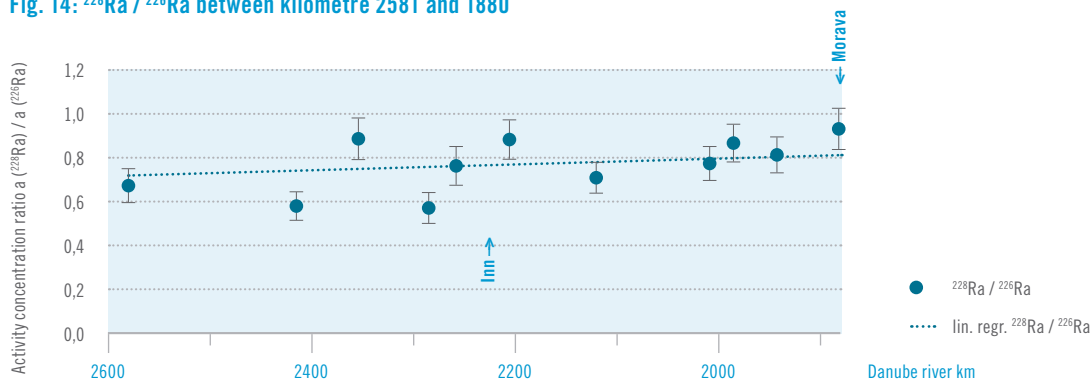


Fig. 15:  $^{228}\text{Ra} / ^{226}\text{Ra}$  between kilometre 1880 and 904

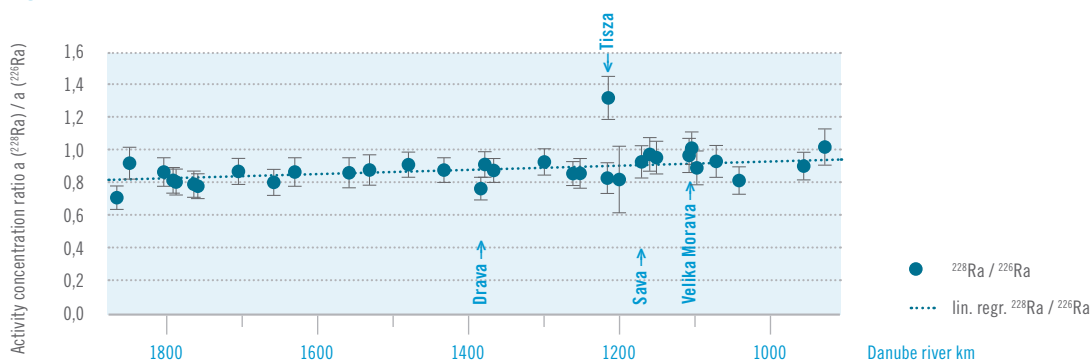
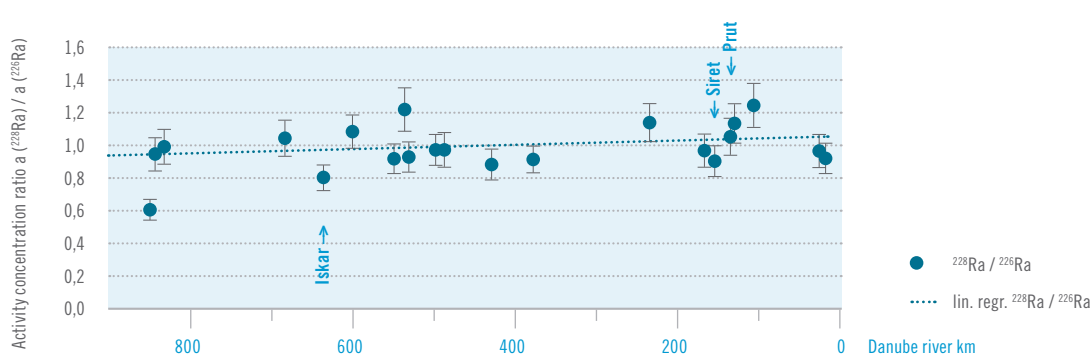


Fig. 16:  $^{228}\text{Ra} / ^{226}\text{Ra}$  between kilometre 904 and 0



### 3.6 Caesium-137 levels between 1988 and 2013

Fig. 17, Fig. 18, and Fig. 19 incorporate data of four different research projects from the years 1988 (Maringer et al., 2009), 2004 (Aquaterra, 2010), 2007 (ICPDR, 2008) and 2013 showing  $^{137}\text{Cs}$  activity concentration levels of Danube sediment. Between 1988 and the subsequent data of 2004, a decrease of one order of magnitude is notable. The results from 2007 align with the previous measurements, but some decrease in activity can be observed. It seems the processes may be best described by an exponential decay.

The measurements conducted in 2013 in the course of *JDS3* show an intermingled progression. The overall results are significantly lower than data acquired six years prior.

Again, the obtained values are lower downstream than at the river source. Notably, the data indicates values have reached concentrations of less than 10 Bq/kg in the lowest section of the river.

Fig. 17:  $^{137}\text{Cs}$  between river kilometre 2600 and 1880 with data from 1988–2013

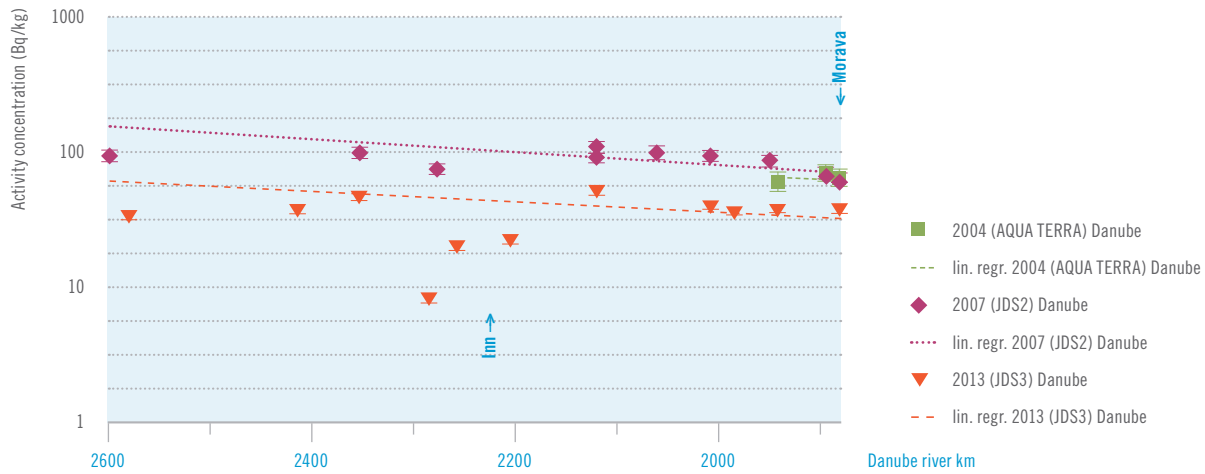


Fig. 18:  $^{137}\text{Cs}$  between river kilometre 1880 and 904 with data from 1988–2013

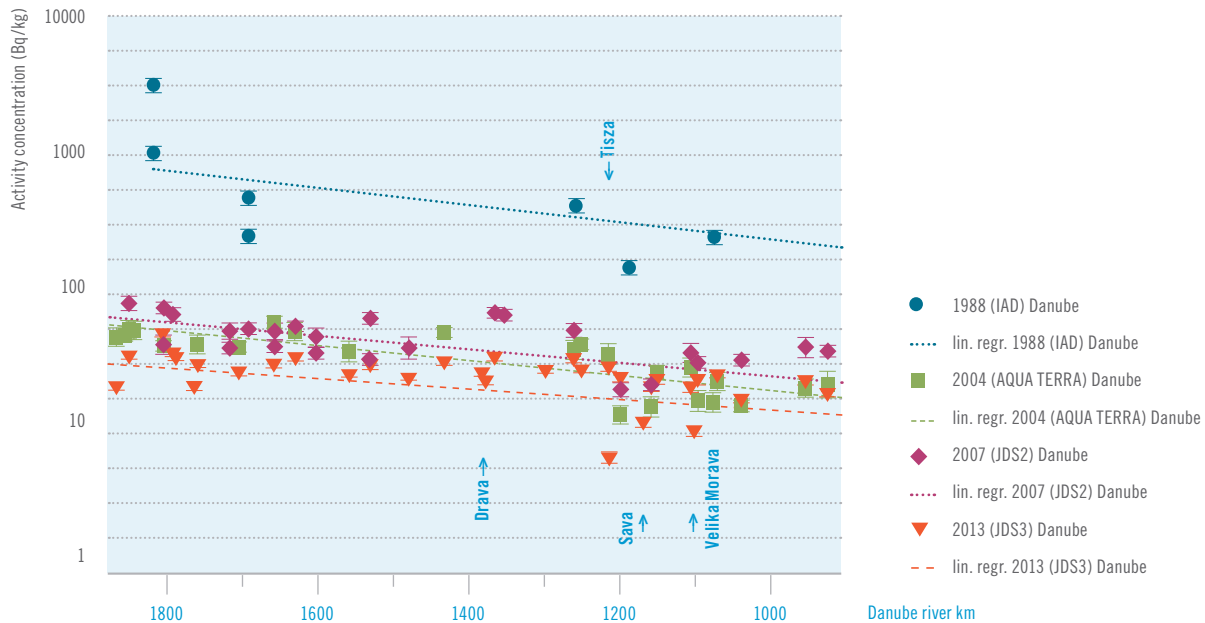
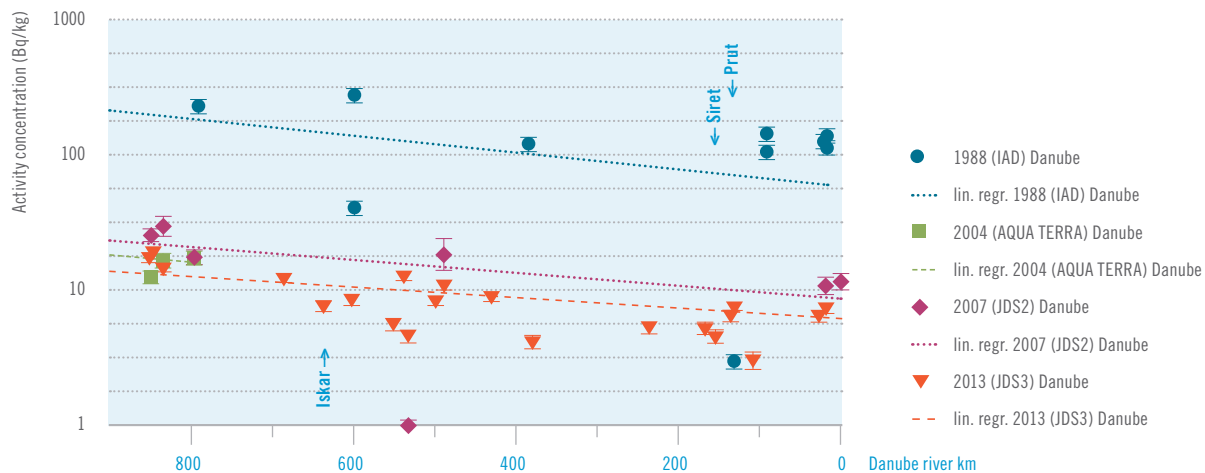


Fig. 19:  $^{137}\text{Cs}$  between river kilometre 904 and 0 with data from 1988–2013

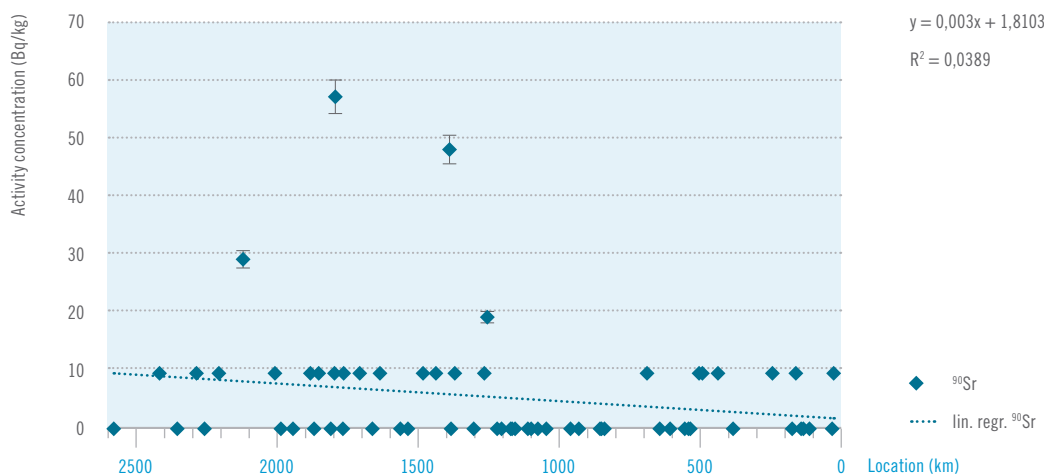


### 3.7 Strontium-90

On average, the specific activities of the analysed sediment samples were found to be about 10 Bq/kg or less apart from some exceptions (Fig. 20). About one third of the samples showed no detectable activity at all (<10 Bq/kg). Most of the  $^{90}\text{Sr}$  at activity concentrations (around 10 Bq/kg) were found in the upper half of the Danube river, more precisely between km 2412 Kelheim (Germany) and km 1252 Novi Sad (Serbia) and from km 498 Rusenski Lom (Bulgaria) also in the Danube Delta. As shown in Fig. 20, there are three regions with higher activity concentration: km 1120 Asten (Germany) with 30 Bq/kg, km 1790 Moson (Hungary) with 57 Bq/kg and km 1384 Dravski Kut (Croatia) with 48 Bq/kg.

Generally, there is an activity decrease of  $^{90}\text{Sr}$  along the river, which results from the flow of the river but also the contamination back than in 1986. When the higher peaks are excluded from the calculation, the slope of the regression is even smaller and decreases from  $0,003 \text{ Bq kg}^{-1} \text{ km}^{-1}$  to  $0,001 \text{ Bq kg}^{-1} \text{ km}^{-1}$ . The surface ground deposition of  $^{137}\text{Cs}$  after the Chernobyl accident from the Danube states shows that Austria, Germany and Romania were affected the most by radioactive deposition. A higher contamination can be expected there since on the Romanian part of the Danube a higher activity concentration was also measured. This could be a possible reason for the higher peaks, when one bears in mind that the maxima migrate with time and with the flow of the river. Due to the several tributaries into the Danube River and therefore increasing water volume, the  $^{90}\text{Sr}$  gets diluted, which is confirmed by the results and the low value for the slope.

Fig. 20:  $^{90}\text{Sr}$  on the entire length of the Danube River



### 3.8 Discussion of Strontium-90 analysis uncertainties

Since the radiochemical extraction and separation processes are laborious with several intermediate steps, it is important to discuss the uncertainties of each step (Steinhauser et al., 2013). The first step was the extraction of strontium from the sediment, in which we found by TXRF-measurements, that with an extraction time of two hours almost complete extraction (98,6%) of the strontium from the samples was possible. Therefore, uncertainty introduced by the extraction step is minimal, so we have to focus on the intermediate steps of the radiochemical process. To be sure that all of the strontium is dissolved, the soil needs to be heated in acid for longer than two hours until complete dissolution, which is not reasonable for so many samples.

The next steps were filtration and evaporation. To make a precise statement regarding the efficiencies, the whole process was carried out with Sr-85. In these steps, a recovery of 87,23% ( $\pm 2,43$ ) is reached, the loss of strontium occurs mainly in the filter. The strontium resins used for the separation had a very good efficiency of about 99% at the first use. All resins used for the analysis of the samples were used only one time. The last step was the LSC-measurement. Since long measuring times of 12 hours were used, the counting statistics uncertainty was very low (below 2%).

The total relative standard measurement uncertainty of the radiochemical  $^{90}\text{Sr}$  analysis is about 10%.





# 4. Conclusions

Eight radionuclides ( $^{40}\text{K}$ ,  $^{90}\text{Sr}$ ,  $^{137}\text{Cs}$ ,  $^{210}\text{Pb}$ ,  $^{226}\text{Ra}$ ,  $^{228}\text{Ra}$ ,  $^{228}\text{Th}$ ,  $^{238}\text{U}$ ) were analysed from 65 bottom sediment samples of the Danube River collected during the *JDS3* in summer 2013. They showed different distributions that were most likely influenced by the variety of rocks present in the river basin as well as many geological, geographical, and anthropogenic influences that exceed the scale of this research.

Notably, the chronological development of the  $^{137}\text{Cs}$  levels gives an insight into the ecological decay of the element and makes it possible to apply a theoretical model that may give a projection on a possible development in the future.

As part of *JDS3*, the given radiometric analysis of the sediment samples provides a representative view on the radioactivity levels of natural ( $^{40}\text{K}$ ,  $^{226}\text{Ra}$ ,  $^{228}\text{Ra}$ ,  $^{228}\text{Th}$ ) and artificial ( $^{137}\text{Cs}$ ,  $^{90}\text{Sr}$ ) radionuclides in the Danube as well as permit further research to be conducted with comparable data in order to be able to detect and interpret changes in years to come, not just for  $^{137}\text{Cs}$  but also for many of the other nuclides.

The decline of  $^{137}\text{Cs}$  concentration in the top sediment layers is caused by reduced  $^{137}\text{Cs}$  concentrations at the source of sediments: due to erosion, the top layers of soil, where most of the  $^{137}\text{Cs}$  was bound, were eroded into rivers, gradually reducing the fresh influx of  $^{137}\text{Cs}$ .

A clear general decrease in the  $^{137}\text{Cs}$  activity concentration of Danube sediments by a factor of 10 was observed between 1988 and 2013. Since 2004 generally a constant  $^{137}\text{Cs}$  level was detected and in the midsection of the Danube rather an increase was found due to downstream transport of remobilised sediment and locally increased  $^{137}\text{Cs}$  input by soil erosion.

The specific activity of  $\beta$ -emitting  $^{90}\text{Sr}$  in sediment samples along the Danube River was determined. This set of observations is of great importance since it is the first one of this type done for the whole Danube River. The  $^{90}\text{Sr}$  contamination levels of the analysed sediment samples were very low and did not exceed 10 Bq/kg with a few exceptions. A decrease in specific activity in sediment along the river was also observed.

Due to the generally decreased artificial radioactivity levels ( $^{90}\text{Sr}$ ,  $^{137}\text{Cs}$ ) in the Danube compartments, no health risk for the population could be deduced. Similarly the natural radionuclide concentrations are at average levels even if large variations of natural radionuclide activity concentrations were observed. This means that the Danube in total was in 2013 in a very good radioecological status.

# 5. References

- Aquaterra, 2010. **BASIN – Integration of Research in AquaTerra River Basins, Chapter 7**. In: Advanced Tools and Models to Improve River Basin Management in Europe in the Context of Global Change – AquaTerra. Ed. M. Finkel, P. Grathwohl, and J. Barth. IWA Publishing, London UK.
- Dossetoa, A., Bourdonb, B. & Turnera, S. P., 2008. **Uranium-series isotopes in river materials: Insights into the timescales of erosion and sediment transport**. *Earth and Planetary Science Letters Volume 265, Issues 1–2*, 15 January, pp. 1–17.
- Eichrom: [www.eichrom.com](http://www.eichrom.com)
- Frantz, A., 1967. **The radioactivity of the Danube**. *Limnology of the Danube*, Volume IV, pp. 84–96.
- Horwitz P. E., Dietz M. L., Fisher D.E, **Separation and Preconcentration of Strontium from Biological, Environmental, and Nuclear Waste Samples by Extraction Chromatography Using a Crown Ether**, *Anal. Chem.* 1991, 63, 522–525
- ICPDR, 2008. **Joint Danube Survey 2. Final Scientific Report, Joint Danube Survey 3**. A Comprehensive Analysis of Danube Water Quality. International Commission for the Protection of the Danube River, Vienna.
- ICPDR, 2015. **Joint Danube Survey 3 - A Comprehensive Analysis of Danube Water Quality**, Vienna: JDS3 Final Scientific Report.
- Kocadag M., Musilek A., Steinhauer G., **On the Interference of Pb-210 in the Determination of Sr-90 Using a Strontium Specific Resin**, *Nuclear Technology & Radiation Protection*, 2013, Vol.28, No 2., pp. 163–168
- Maringer, F. et al., 2009. **Long-term monitoring of the Danube river – Sampling techniques, radionuclide metrology and radioecological assessment**. *Applied Radiation and Isotopes 67*, pp. 894–900.
- Mundschenk H., **Verfahren zur Bestimmung von Strontium-98 und Strontium-90 in Oberflächenwasser im Normalfall, Leitstelle für Oberflächenwasser, Schwebstoff und Sediment in Binnengeässern**, 1994, ISSN 1865-8725
- National Institute of Standards and Technology, 2016a. **Basic Atomic Spectroscopic Data**. [Online] Available at: <http://physics.nist.gov/PhysRefData/Handbook/Tables/potassiumtable1.htm> [Accessed 30 September 2016].
- National Institute of Standards and Technology, 2016b. **New Standardization of Ra-228**. [Online] Available at: <https://www.nist.gov/programs-projects/new-standardization-ra-228> [Accessed 1 October 2016].
- National Institute of Standards and Technology, 2016c. **Radionuclide Half-Life Measurements Data**. [Online] Available at: <https://www.nist.gov/pml/radionuclide-half-life-measurements> [Accessed 30 September 2016].
- Pimpl M., **89Sr/90Sr-Determination in soils and sediments using crown ethers for Ca/Sr-separation**, *Journal of Radioanalytical and Nuclear Chemistry*, 1995, Vol. 194, Issue 2, pp 311–318
- Steinhauer G., Schauer V., Shozugawa K., **Concentration of Strontium-90 at Selected Hot Spots in Japan**, *PLOS ONE*, 2013, 8(3):e57760. Doi:10.1371
- Rank, D., 1976. **Measurement of tritium and radio-carbon in the environment**. *OESRAD-Meeting*.
- Tschurlovits, M., Buchtela, K., Sas-Hubicki, J. & Unfried, E., 1980. **Determination of Cs-137, Sr-90 and gamma spectroscopy of water samples from the Danube river**. *IAEA-TECDOC-229*, pp. 9–22.



